

# Adaptive Mesh Refinement for 1-D Hyperbolic PDEs

Saumya Sinha\*, Kenneth J. Roche†

March 14, 2015

**Abstract:** We describe an adaptive mesh refinement algorithm that extends high resolution wave-propagation techniques to hyperbolic systems in non-conservative form. The method for keeping numerical conservation at grid cell interfaces is described. The algorithm was tested for simple 1D problems. Results are compared to static mesh solutions for the same problems.

## Contents

<b>1</b>	<b>Introduction</b>	<b>2</b>
<b>2</b>	<b>The AMR algorithm</b>	<b>2</b>
2.1	Advance solution over coarse grid . . . . .	2
2.2	determining refinement - error estimation . . . . .	3
2.3	assigning values to new fine grid points . . . . .	4
2.4	updates on refined and coarse meshes . . . . .	4
2.5	updating grid interfaces with wave propagation -correction step . . . . .	5
2.6	AMR algorithm . . . . .	6
<b>3</b>	<b>Examples of 1D AMR</b>	<b>7</b>
3.1	variable coefficient . . . . .	7
<b>4</b>	<b>Software implementation</b>	<b>8</b>
<b>5</b>	<b>Summary</b>	<b>8</b>

---

\*Department of Applied Mathematics, University of Washington, Seattle, Washington U.S.A. Email:saumya@uw.edu

†High Performance Computing Group, Pacific Northwest National Laboratory, 1 Battelle Road, Richland, Washington U.S.A. Email:kenneth.roche@pnnl.gov

# 1 Introduction

We describe an adaptive mesh refinement (AMR) strategy for the solution of hyperbolic systems of conservation laws. The solutions of these equations are often smooth and easily approximated over large portions of their domain, but contain locally isolated regions with steep gradients, shocks or discontinuities. Our AMR strategy models and tracks such regions, by using rectangular patches over Cartesian grids to refine both the space and time coordinates.

## 2 The AMR algorithm

In this paper, we consider only one-dimensional systems. The coarse grid consists of a collection of intervals or cells that cover the entire domain, while refinements cover a subset of the domain and have finer cell-widths. If the cell-width in a fine grid is refined by an even integer  $R_L$ , then the time-step is also refined by the same factor, so that the ratio  $\Delta t/\Delta x$  remains unchanged and for every single time-step on the coarse grid,  $R_L$  time steps must be taken on the fine grid.

An error estimation procedure based on Richardson extrapolation, described in more detail in section 2.2, is used to flag the cells which need refinement. Flagged cells are clustered into patches, and a fine grid is generated for each patch (including a buffer zone). A finite volume method in wave-propagation form is used to advance the solution on the coarse grid over a single time-step, and then the solution on the fine grid(s) is advanced over  $R_L$  time steps to catch-up.

Every  $K$  time steps ( $K$  is related to the number of buffer cells retained), the fine grids are regenerated, and the error estimation procedure is re-applied to capture the movement of the discontinuities. The refinement and solution process is repeated.

Each of the above steps is described in more detail below.

### 2.1 Advance solution over coarse grid

After initializing the discrete coarse grid, the first step is to advance the solution over a single time-step on the coarse grid. We have implemented a standard high resolution wave propagation method (with limiter corrections) to solve the Riemann problem.

To clarify, consider a linear system  $q_t + A(x)q_x = 0$  where  $q \in \mathbb{R}^m$  and  $A \in \mathbb{R}^{m \times m}$  is diagonalizable with real eigenvalues. On the cell  $[x_{i-1/2}, x_{i+1/2}]$ , the matrix  $A(x)$  is approximated by a matrix  $A_{i-1}$  with eigenvalues  $\lambda_{i-1}^1, \dots, \lambda_{i-1}^m$ . Then for the Riemann problem at  $x_{i-1/2}$ , we decompose  $q_i - q_{i-1}$  into waves  $\mathcal{W}_i^p, p = 1, 2, \dots, m$  in such a way that the left-going waves are eigenvectors of the matrix  $A_{i-1}$ , traveling with speeds  $\lambda_{i-1}^p < 0$ , while the right-going waves are eigenvectors of  $A_i$  traveling with speeds  $\lambda_i^p > 0$ . The update formula is then

$$(1) \quad q_i^{n+1} = q_i^n - \frac{k}{h} \sum_{p=1}^m [(\lambda_i^p)^+ \mathcal{W}_i^p + (\lambda_{i+1}^p)^- \mathcal{W}_{i+1}^p] - \frac{k}{h} (\tilde{F}_{i+1} - \tilde{F}_i)$$

where  $k$  is the length of the time-step and  $h$  is the cell-width in the spatial grid, and for any real number  $a$ ,  $a^+ = \max\{a, 0\}$  and  $a^- = \max\{-a, 0\}$ .

The summation term gives the first-order upwind method, while the fluxes  $\tilde{F}_i$  are the second-order corrections defined by

$$(2) \quad \tilde{F}_i = \frac{1}{2} \sum_{p=1}^m |\lambda_i^p| \left( 1 - \frac{k}{h} |\lambda_i^p| \right) \tilde{\mathcal{W}}_{i+1}$$

where  $\tilde{\mathcal{W}}_{i+1}^p$  is some limited version of the wave  $\mathcal{W}_i^p$ . When  $\tilde{\mathcal{W}}_i = \mathcal{W}_i$ , the method is reduced to upwind + second order correction, i.e. Lax-Wendroff method.

This method is extended to nonlinear systems using the Roe approximate Riemann solver, which linearizes the problem at each cell-interface in such a way that conservation is guaranteed. This method is symbolically written as

$$q_i^{n+1} = q_i^n - \frac{k}{h} \sum_{p=1}^m [\mathcal{A}^+ \Delta(q_i) + \mathcal{A}^- \Delta(q_{i+1})] - \frac{k}{h} (\tilde{F}_{i+1} - \tilde{F}_i)$$

where  $\mathcal{A}^+ \Delta(q_i)$  represents the right-going fluctuation from the left interface of cell  $i$ , while  $\mathcal{A}^- \Delta(q_i)$  is the left-going fluctuation from the right interface of cell  $i$ .

## 2.2 determining refinement - error estimation

At the core of the refinement step is determining where a refinement may be useful. If the solution  $q(x, t)$  is smooth enough, we assume that method  $D$  (application of eqn(9)) has accuracy  $O(s)$  in both space and time. The local truncation error is  $q(x, t+k) - Dq(x, t) = \tau(x, t) + kO(k^{s+1} + h^{s+1})$  where  $\tau$  is the leading error. Taking two time steps suggests  $q(x, t+2k) - D^2q(x, t) = 2\tau(x, t) + kO(k^{s+1} + h^{s+1})$ . Now, coarsen the grid to have space and time widths  $2h, 2k$  and let the differencing scheme be called  $D_{2h}$  in this case. The local truncation error in this case reads  $q(x, t+2k) - D_{2h}q(x, t) = 2^{s+1}\tau(x, t) + O(h^{s+2})$ . Thus, an error growth estimate at time  $t$  can be formed by taking the difference in the error taking two steps with the regular integration scheme, and a single large step using every other grid point:

$$(3) \quad \frac{D^2q(x, t) - D_{2h}q(x, t)}{2^{s+1} - 2} = \tau(x, t) + O(h^{s+2}).$$

The difference between the solutions obtained on the two grids at each point is proportional to the local truncation error at that point. At coarse cells where the difference between the two sets of values exceed some tolerance, all four cells contained in the real grid are flagged as requiring refinement. See [3] for more details. *Clustering* is simply to fill gaps in neighboring cells flagged for refinement. For instance, should there be a single cell not flagged for refinement between cells that require refinement, the cell in between will be refined as well and the adjacent clusters are merged into a single larger cluster. A buffer zone around the flagged cells is added to track features of interest in the refined region and to enable taking  $K > 1$  steps prior to regridding. This buffer zone must be affiliated with the number of time steps evaluated at a particular level. If a patch at level  $L$  is refined by even integer  $R_L$ , then the time-step is equally refined implying that  $R_L$  steps must be taken on the refined grid at level  $L+1$  for each step on grid at level  $L$ .

### 2.3 assigning values to new fine grid points

Once regions where a fine grid are determined, values must be assigned to the fine grid points. Space-time interpolation is needed to supply values for the fine grid because more time steps are taken on the fine grid than the coarse grid and there are no coarse grid values available at intermediate times. This is achieved through a linear interpolation step with known coarse grid values at the current time level and these values are available since we advance the coarse grid first as stated in the algorithm.

### 2.4 updates on refined and coarse meshes

After finishing the recursive step creating the fine grid structure and initializing grid values for the current time, how to evolve the grid levels needs to be considered. To evolve, conservation of fluxes at grid interfaces is required. We refer to Fig 1 for this discussion. There are essentially three cases to consider: coarse cell to coarse cell, fine cell to fine cell, and overlapping coarse cell and fine cell regions. Let  $F_i$  be the flux at the left edge of coarse cell  $i$  at time  $n$ . This is different notation than what we typically wrote in class,  $F_{i-\frac{1}{2}}$ .

Updating between coarse grid cells is achieved by evaluating the method a single step, i.e. to lowest order:

$$(4) \quad q_i^1 = q_i^0 - \frac{k}{h}(F_{i+1}^0 - F_i^0)$$

where  $h, k$  are the space and time lattice spacing respectively.

In regions that contain  $m$  adjacent single level refined cells let the lattice spacing be denoted by  $\hat{h}, \hat{k}$ . We again solve by evaluating the method noting that at each intermediate level the evaluation may invoke values in neighboring cells of the same level or ghost cells defined for the level. We have then,  $\forall i = 1, m$  :

$$(5) \quad \begin{aligned} \hat{q}_i^1 &= \hat{q}_i^0 - \frac{\hat{k}}{\hat{h}}(\hat{F}_{i+1}^0 - \hat{F}_i^0) \\ \hat{q}_i^2 &= \hat{q}_i^1 - \frac{\hat{k}}{\hat{h}}(\hat{F}_{i+1}^1 - \hat{F}_i^1) \end{aligned}$$

in the refined cells where for simplicity we assume  $R = 2$ .

In regions where the coarse and fine grids overlap, care must be taken. Ghost cells are introduced,  $\hat{q}_{m+1}, \hat{q}_{m+2}$ . The values in these cells at intermediate times are decided by evaluating a polynomial (determined by interpolating the known coarse values that enclose the unknown values) at these fine grid locations. At the final time (completed time step)  $q_i^1$  is replaced by the average of the fine grid values in the overlapped region:

$$(6) \quad q_{j-1}^1 = \frac{1}{2}(\hat{q}_{m+1}^2 + \hat{q}_{m+2}^2)$$

and the corresponding left edge flux is similarly modified so that  $q_i^1$  is finally modified as:

$$(7) \quad q_i^1 \rightarrow q_i^1 + \frac{k}{h}(\frac{1}{2}(\hat{F}_{m+1}^0 + \hat{F}_{m+1}^1) - F_i^0).$$

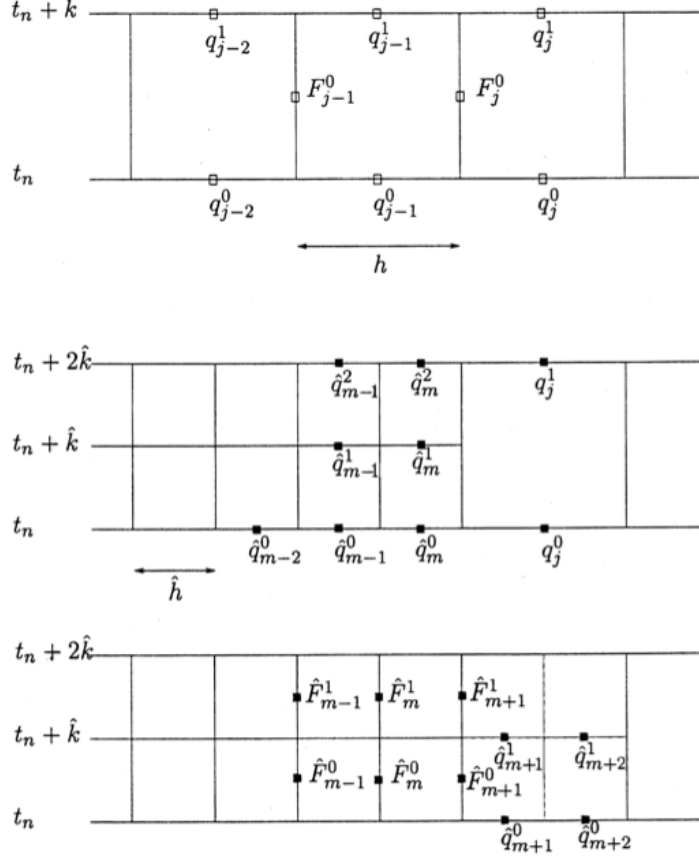


Figure 1: Essential figure for flux adapting Cartesian grids. The top grid is the normal coarse grid we are used to using with fluxes indicated. The middle diagram shows the case where a fine grid overlays a coarse grid and the interface region of fine and coarse grids. Recall that  $2\hat{h} = h$  and  $2\hat{k} = k$ . The bottom diagram depicts the ghost cell region imposed on the coarse cell interface as well as the fine grid fluxes needed to bridge the interface.

## 2.5 updating grid interfaces with wave propagation -correction step

With flux-differencing to ensure conservation, a new coarse grid value is updated by an average of fine-grid values in any cell covered by a fine grid. The key to conservation is that flux into coarse cells is accounted for by flux out of adjacent fine cells, and vice versa, as described in the previous section. Wave propagation algorithms are written in a manner that they can be extended to hyperbolic problems not in conservation form retaining wave features but with no flux function. For wave-propagation algorithms, a similar correction is needed for the waves to yield conservation. The wave-propagation form can be used to update the values at the interface between fine and coarse grid cells on each grid independently using ghost-cell values as needed near grid interfaces. This is exactly what we have done.

Recall from class that  $A^+ \Delta q_{i-\frac{1}{2}}$  is a symbol intended to indicate the net effect of all right going waves present from  $x_{i-\frac{1}{2}}$ , and  $A^- \Delta q_{i-\frac{1}{2}}$  measures the net effect of all left going waves from the same interface. We call these *fluctuations*. Whether conservative or non-conservative systems are treated, second-order corrections are still written as flux-differences. However, the

first-order upwind terms written in terms of the fluctuations must be handled differently. To maintain conservation we must *first* solve the Riemann problem between the ghost cell value  $\hat{q}_{m+1}^0$  on the fine grid and the coarse grid value  $q_j^0$ , and add to the coarse cell value  $q_j^1$  the resulting total fluctuation (dropped indices)  $A^-\Delta q + A^+\Delta q$  weighted by  $\hat{k}/h = 1/2$  since the time step is  $\hat{k}$  while the cell size is  $h$ . *Second* we must also solve a Riemann problem on the fine grid between  $\hat{q}_{m+1}^1$  and  $q_j^0$  and add these fluctuations into  $q_j^1$ .

The correction step extends to an arbitrary hyperbolic systems where we use a Riemann solver to obtain  $A^-\Delta q$  and  $A^+\Delta q$  from the two states  $\hat{q}_{m+1}^0$  and  $q_j^0$ . This step is made in each of the  $R$  time steps on the refined grid within the single coarse-grid step, where  $R$  is the refinement ratio.

In summary, the correction algorithm reads:

**for**  $N = 0, R - 1$

solve the Riemann problem with data  $\hat{q}_{m+1}^N$  and  $q_j^0$  to compute  $A^-\Delta q$  and  $A^+\Delta q$

update  $q_j^1 \rightarrow q_j^1 + \frac{\hat{k}}{h} (A^-\Delta q + A^+\Delta q)$

## 2.6 AMR algorithm

We present in the section a fairly detailed

Steps for the AMR algorithm:

- (a) initialize coarsest grid (called level  $i = 0$ )
- (b) *recurse*: if level ( $i > levels_{max}$ ) *break*
  - flag cells for current level  $i$ 
    - estimate error in each level  $i$  cell (compare  $D^2(i), D_{2h(i)}$ )
      - \* if error condition violated, bump *flagged*
  - if (*flagged* > 0) construct level  $i + 1$  grid
    - cluster (based on buffer region and ghost cells) level  $i$  grid cells
    - initialize  $i + 1$  grid for current time
      - \* linear interpolation using level  $i$  values at current time
  - $i \leftarrow i + 1$
- (c) partial time evolution
  - $\forall levels(i)$  take single  $dt(level(i))$  step by evaluating method
    - at fine-coarse interfaces evaluate points at  $dt(level(i))$  time
      - \* requires interpolating function formed with bilinear interpolation with  $level(i-1)$  values
      - \* **comment:** telescoping step that ends up depending on level  $i = 0$  solutions
- (d) promote grid solutions per grid level to full time step

- $\forall i = L, 1$   $level(i)$  updates interior cells at  $level(i - 1)$ 
  - evaluate method using  $level(i)$  points and average to form value
- correction step to ensure conservation at fine-coarse interfaces
  - sequentially solve Riemann problems between  $level(i)$  values closest to interface and value at  $level(i - 1)$
  - after each solve, contribution is added to value at  $level(i - 1)$

(e) completes single time step on coarse grid  $level(0)$ , go to step  $b$

Here we let  $dt(level(i)) = \frac{dt(0)}{R_{level(i)}}$  where  $R_{level(i)} = 2^i$ ,  $dx(level(i)) = \frac{dx(0)}{R_{level(i)}}$ , and  $0 \leq L \leq levels_{max}$ , the maximum level refinement reached. The major steps are depicted pictorially in table 2.6.

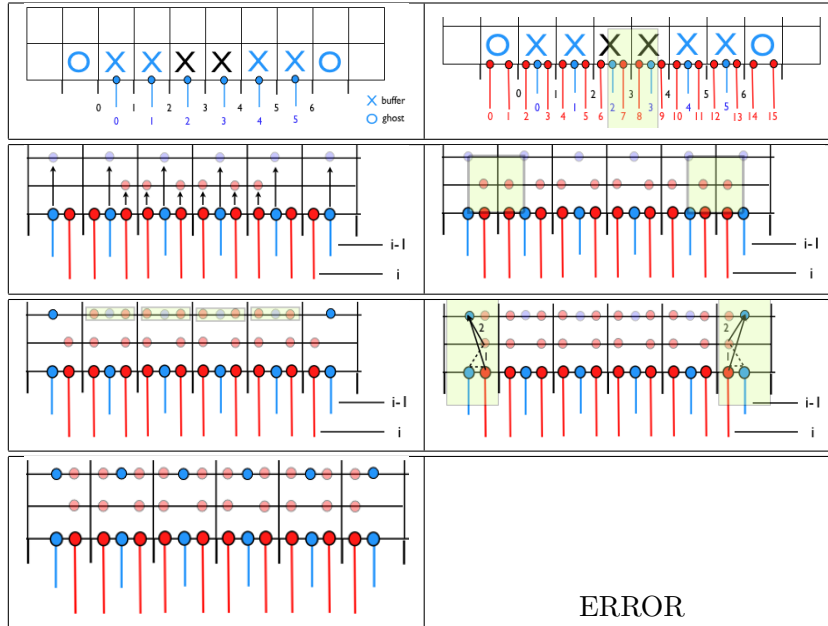


Table 1: AMR(b): (1,1) flag cells and introduce buffer zone and ghost cells. (1,2) cluster and interpolate for current time level values on fine grid. AMR(c): (2,1) single  $dt(level(i))$  step, coarse and interior fine grid cells only. (2,2) complete single step for fine grid at coarse-fine interfaces using bilinear interpolation and function evaluation. AMR(d): (3,1) full time step -average interior cells to evaluate coarse cell average for  $t_{n+1}$ . (3,2) at coarse-fine interfaces solve Riemann problems  $(\hat{q}_i^0, q_i^0), (\hat{q}_i^1, q_i^0)$  and add contribution to coarse cell value (scaled by  $q_i^1$ ). AMR(e): (4,3) all grids ready for  $K$  step advance. ERROR: Please note that the red dots in ghost cells at  $t_{n+1}$  are not supposed to be there. They will be updated but not until next AMR(b) step.

### 3 Examples of 1D AMR

#### 3.1 variable coefficient

Here we state a 1D scalar problem based on a variable coefficient velocity term. We studied this equation in our efforts to implement 1D AMR. The *color* equation is the problem formed by solving the following Riemann problem at the interface  $x_{i-\frac{1}{2}}$  between cells  $i-1$  and  $i$ :

$$(8) \quad q(x, t)_t + u(x)q(x, t)_x = 0$$

The method reads, i.e. for the *color* eqn (see 3.1):

$$(9) \quad q_i^{n+1} = q_i^n - \frac{k}{h}(u_i^+(q_i^n - q_{i-1}^n) + u_i^-(q_{i+1}^n - q_i^n)) - \frac{k}{h}(\tilde{F}_{i+1} - \tilde{F}_i)$$

where

$$(10) \quad \tilde{F}_i = \frac{1}{2}|u_i|(1 - \frac{k}{h}|u_i|)\tilde{W}_i$$

and the limiter is applied to wave  $W_i = q_i - q_{i-1}$  i.e. traveling at speed  $u(x)$ , such that

$$(11) \quad \tilde{W}_i = \begin{cases} \text{limiter}(W_i, W_{i-1}), & u_i > 0 \\ \text{limiter}(W_i, W_{i+1}), & u_i < 0 \end{cases}$$

$$(12) \quad q(x, 0) := \phi(x) = \begin{cases} q_{i-1}, & x < x_{i-\frac{1}{2}} \\ q_i, & x > x_{i-\frac{1}{2}} \end{cases}, \quad u(x) = \begin{cases} u_{i-1}, & x < x_{i-\frac{1}{2}} \\ u_i, & x > x_{i-\frac{1}{2}} \end{cases}$$

and the sign of  $u(x)$  arbitrary for now.

### 4 Software implementation

Rather than invoking Clawpack[1] which does everything quite nicely already, we implemented our own numerical Riemann solvers to test our AMR developments in apples to apples fashion. We have successfully implemented the static refinement case for arbitrary  $R = 2^k$ ,  $k$  some integer  $\geq 0$ . The Python software for simple level 1 refinement was reproduced in C, but the C code to fully implement recursive refinement is not functioning correctly and we fell short on time for this report to finish debugging despite big efforts. We note that studies comparing the performance of refining a fixed mesh solution globally to our software that selectively identifies regions to refine would be important. AMR is memory intensive and the tradeoffs are worth understanding. Other factors that influence the outcome of the value of AMR are related to the number of buffer zone cells kept, clearly the level of refinement enabled, the evaluation of the error criterion, etc. We did not come close to fully understanding the correct selection of parameters for our implementation. However, please see figure 2, the implementation does correctly refine regions of discontinuous or sharp solution behaviors. The CFL condition became relevant for several of the problem cases we have tested.



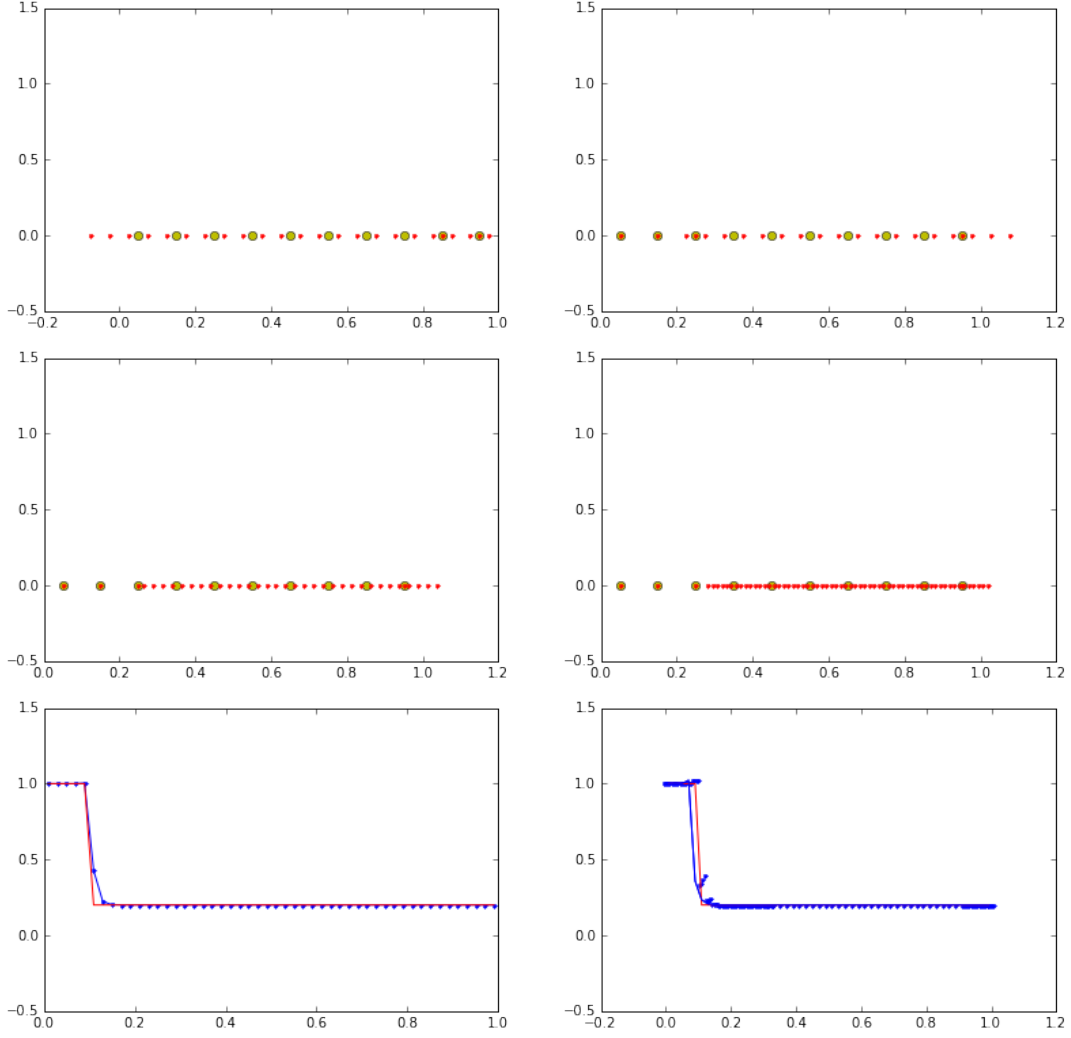


Figure 2: (top row) single level refinement,  $R = 2$  at  $t_0$ ,  $t_f$ . (middle) single level refinement,  $R = 4$  and  $R = 8$  at  $t_f$ . (bottom)  $u = x^2$  profile for no (left) amr and with (right) amr.

## 5 Summary

In this paper we described the adaptive mesh refinement algorithm presented in [4], and implemented the non-recursive formulation and tested the method for several simplistic 1D cases.

## References

- [1] <http://www.clawpack.org>
- [2] R. Leveque Finite Volume Methods for Hyperbolic Problems Cambridge University Press (2002)
- [3] M. Berger and P. Collela, Local Adaptive Mesh Refinement for Shock Hydrodynamics Journal of Computational Physics 82, 64-84 (1989)
- [4] M. Berger and R. Leveque, Adaptive Mesh Refinement Using Wave-Propagation Algorithms for Hyperbolic Systems SIAM Journal of Numerical Analysis, 35(6):2298–2316, (1998)
- [5] M. Berger, Adaptive Mesh Refinement for Hyperbolic Partial Differential Equations, *PhD Thesis*, Department of Computer Science, Stanford University, Stanford, CA 94305 (1982)